TU/e EINDHOVEN UNIVERSITY OF TECHNOLOGY

Apparent charge magnitude in on-line PD diagnostics on medium-voltage power cables

Citation for published version (APA):
Wouters, P. A. A. F., Li, Y., Mousavi Gargari, S., Wagenaars, P., & Steennis, E. F. (2011). Apparent charge magnitude in on-line PD diagnostics on medium-voltage power cables. In *Proceedings of the 17th International Symposium on High Voltage Engineering (ISH 2011), August 22-26 2011, Hannover, Germabny*

Document status and date:
Published: 01/01/2011

Document Version:
Publisher's PDF, also known as Version of Record (includes final page, issue and volume numbers)

Please check the document version of this publication:

• A submitted manuscript is the version of the article upon submission and before peer-review. There can be important differences between the submitted version and the official published version of record. People interested in the research are advised to contact the author for the final version of the publication, or visit the DOI to the publisher's website.
• The final author version and the galley proof are versions of the publication after peer review.
• The final published version features the final layout of the paper including the volume, issue and page numbers.

Link to publication

General rights
Copyright and moral rights for the publications made accessible in the public portal are retained by the authors and/or other copyright owners and it is a condition of accessing publications that users recognise and abide by the legal requirements associated with these rights.

• Users may download and print one copy of any publication from the public portal for the purpose of private study or research.
• You may not further distribute the material or use it for any profit-making activity or commercial gain
• You may freely distribute the URL identifying the publication in the public portal.

If the publication is distributed under the terms of Article 25fa of the Dutch Copyright Act, indicated by the "Taverne" license above, please follow below link for the End User Agreement:

www.tue.nl/taverne

Take down policy
If you believe that this document breaches copyright please contact us at:

openaccess@tue.nl

providing details and we will investigate your claim.

Download date: 16. Oct. 2021

APPARENT CHARGE MAGNITUDE IN ON-LINE PD DIAGNOSTICS ON MEDIUM-VOLTAGE POWER CABLES

P.A.A.F. Wouters[1*], Y. Li[1], S. Mousavi Gargari[1], P. Wagenaars[2], E.F. Steennis[1,2]
[1]Eindhoven University of Technology, the Netherlands
[2]KEMA Nederland B.V., the Netherlands
*Email: <p.a.a.f.wouters@tue.nl>

Abstract: Estimating PD charge magnitude by comparing the response on a real PD and the response on an injected calibration signal with known magnitude in terms of apparent charge is usually not feasible for on-line monitored power cables. The injection cannot take place at a representative position in the cable but only at the cable end, whereas the PD can arise at any position within the cable. Additionally, the PD calibrator should be connected to an energised cable. PD magnitude is viable information if behaviour of similar defects in different cable circuits is to be compared. The present paper discusses a charge estimate method for on-line monitored cables. The method is based on modelling the complete chain of events, i.e. from PD signal excitation at the defect location via its propagation along the cable connection up to detection of the PD signal. By adding a pulse signal injection circuit to the sensors at both cable ends, relevant parameters for modelling the PD signal can be extracted. Monitoring long cable connections is economic attractive but signal loss limits the sensitivity in terms of minimum detectable apparent charge. This issue is discussed on basis of a monitored cable connection over 5.5 km long.

1 INTRODUCTION

Different techniques are nowadays available to detect Partial Discharges (PD) activity for many components applied in the electricity network. To compare the severity of the PDs, their magnitude must be quantified. In testing high-voltage components the sensor response upon a PD is calibrated by comparison with the response upon an injected charge with known magnitude, e.g. [1]. For complex components, e.g. power transformer or generator, this method is not straightforward, since measured PD signals depend on their origin within the component, which usually cannot be assessed by a PD calibrator. The detected signal magnitude depends on defect location, signal propagation path, and sensor characteristics. A similar problem arises in case of on-line diagnostics applied to less complex systems, like a power cable circuit. Also here direct assessment of the PD origin for calibration is not possible. Moreover, an energised power cable complicates safe connection of a calibration unit.

An alternative calibration method is to analyse the complete chain of events associated with a PD signal, i.e. from its excitation at the defect location via its propagation path up to the signal detection [2]. Only after modelling all aspects, a transfer function can be established, which allows estimating the PD magnitude from the detected signal waveform. At the PD location, the associated charge displacement in the cable insulation induces an apparent charge in the cable conductors, from which the PD signal starts to propagate. Next, during propagation, power cable characteristics and components placed in the circuit will affect the transferred PD signal. Finally, the PD signal is transmitted into the Ring Main Unit (RMU) or the substation where a sensor is installed. The recorded waveform depends on sensor characteristics, sensor position within RMU/substation, and installed RMU/substation equipment.

In Section 2 the sequence of events, from PD excitation at the defect up to its detection at the cable end, is analysed. Section 3 describes a method to extract parameters relevant for a cable circuit, where PD signals are detected by means of coils at both ends of a medium-voltage cable connection ending at RMUs. The consequences of PD signal loss in complex cable connections is discussed in Section 4 and an example obtained with a long cable circuit is presented in Section 5. A discussion on the feasibility of the calibration method is given in Section 6.

2 PD SIGNAL TRANSFER

Partial discharge signal initiation, propagation and detection are discussed in the sections below. An apparent charge induced at the defect location will eventually result in a measured signal at the cable ends. With knowledge of all transfer parameters involved, the content of the detected signal can be related to the apparent charge at the PD origin, effectively calibrating the PD magnitude.

2.1 PD initiation

A partial discharge induces a charge Q_{app} in the conductors. For lumped components this can be

probed in tests, e.g. by a parallel RLC impedance of which the response is proportional to Q_{app}. For cables, the PD results in a travelling wave which can be measured at either cable end. The charge moving to each end is ½Q_{app}, provided that the wave at its origin experiences equal characteristic impedances to both sides. The duration of a PD is on nanosecond scale, i.e. significantly shorter than timescales corresponding to the bandwidth applied for PD detection in power cables. Therefore, the waveform at the PD origin, z=0, can be regarded as a Dirac pulse taken at t=0:

$$i_{PD}(t,0) = \tfrac{1}{2} Q_{app} \delta(0) \qquad (1)$$

In frequency domain, the PD energy content spreads over a wide frequency range up to hundreds of MHz [3].

2.2 PD propagation

Power cables are designed for carrying large currents at medium or high voltages. Additional cable layers are incorporated to handle electric stresses, to prevent water ingress or to supply mechanical strength. These layers can have negative effects on the propagation of PD signals. Assuming an excitation with total charge Q_{app}, the PD current in frequency domain after propagating over distance z in one direction is given by:

$$I_{PD}(\omega, z) = I_{PD}(\omega,0)\, \mathrm{e}^{-\gamma(\omega) z} \quad \text{with} \quad I_{PD}(\omega,0) = \tfrac{1}{2} Q_{app} \qquad (2)$$

The propagation coefficient γ(ω) includes the signal attenuation and propagation velocity. A simulation of a PD signal based on values of the propagation coefficient measured on a buried 809 m, 10 kV PILC cable is shown in Figure 1 (top). Both time-domain pulse shape and its frequency content are given after propagation over 300 m, 1 km and 3 km. In the low MHz range the f_{-3dB} for PD detection scales roughly inversely proportional with the cable length ℓ having, as a rule of thumb, a product $f_{-3dB} \cdot \ell \approx 0.3$ MHz km. For XLPE the losses are less. Figure 1 (bottom) shows the pulse using the propagation coefficient measured on a 138 m, 10 kV single-phase XLPE cable on a drum. A product $f_{-3dB} \cdot \ell \approx 1$ MHz km is obtained. These values limit the maximum cable length, since accurate location (in the order of tens of metres) of defects, from signals only containing frequency contents clearly below 1 MHz, is not possible. For a cable connection consisting of sections with cable segments having different characteristic impedances or being interrupted by RMUs, signal reflection contributes to a reduction of the signal fraction that is directly transmitted.

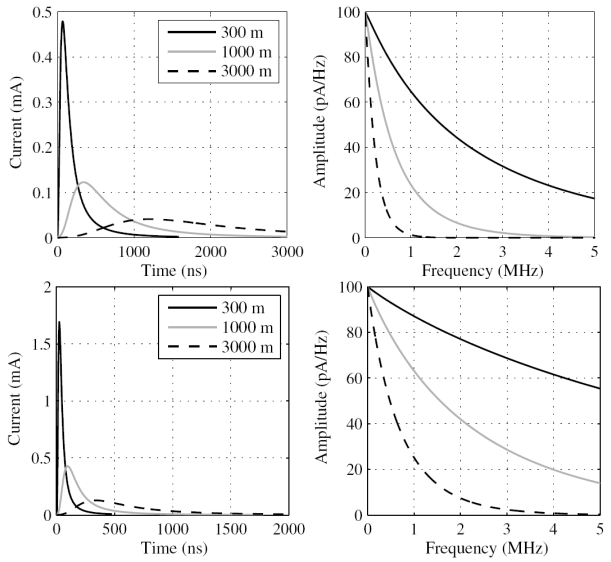

Figure 1: Calculated time-domain and frequency-domain response on a 100 pC pulse propagated along PILC cable (top) and XLPE cable (bottom).

2.3 PD detection

Figure 2 shows an equivalent circuit for a cable which ends in an RMU. The size of the RMU is considered to be sufficiently small to be described as lumped impedance Z_{load}. This complex impedance includes all components, such as outgoing cables, distribution transformers, and inductances due their connections to the busbar. The PD signal detected by the sensor depends on the fraction of the signal that is transmitted into the RMU and on the characteristics of the sensor. The transfer function distorts the signal waveform due to the complex RMU impedance.

In the analysis, it will be assumed that signal coupling takes place inductively by means of coils (see Section 3). Coupling through installed capacitors is an alternative option, but has the disadvantage of requiring galvanic contact to energised parts, which is undesirable for on-line applications. Earlier research [4] has revealed two interesting places for installation of the coils. The power cable is connected to earth at one or more places inside the RMU. If the detection coil is positioned around the "Last Earth Connection" (LEC), the transmitted PD signal is detected. However, since this connection may contribute to the circuit's self-inductance, part of the current may return to the cable screen at other earth connections, indicated by Z_x. A preferred installation position, often available, is around the cable screen "Past the Last Earth Connection"

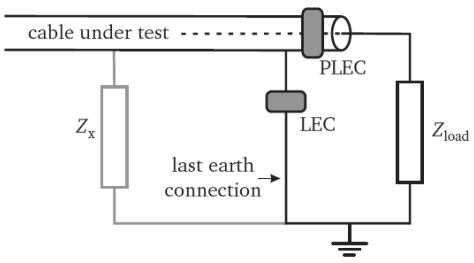

Figure 2: Equivalent model of load by RMU on cable with parallel earth connections; preferred sensor positions are indicated.

(PLEC). Here, the full transmitted current is detected, irrespective of the current return path. Since the cable earth screen is still present there, safe sensor installation even on an energised cable is in principle possible. Also interference from external sources is lower at the PLEC position [4, 5]. The current transmission coefficient $T(\omega)$ from cable, with characteristic impedance Z_c, to the RMU is equal to $2Z_c/(Z_c+Z_{load})$.

The inductive sensor is assumed to have response $Z_{sens}{\cdot}f(\omega)$. Commercial coils are designed for constant transfer Z_{sens} from enclosed current to their output voltage. The function $f(\omega)$ takes into account that for low frequency the sensor sensitivity drops, suppressing the power frequency component. Additional filtering can be incorporated to further eliminate the power frequency component and to remove disturbances outside the frequency range relevant for PD detection in power cables. The sensor output becomes:

$$V(\omega) = Z_{sens} \cdot f(\omega) \cdot T(\omega) \cdot I_{PD}(\omega, z) \tag{3}$$

The charge Q_{sens} contained by the detected signal is defined as:

$$\begin{aligned} Q_{sens} &= \frac{1}{Z_{sens}} \int FT^{-1}\big(V(\omega)\big)dt \\ &= \int FT^{-1}\big(f(\omega) \cdot T(\omega) \cdot I_{PD}(\omega, z)\big)dt \end{aligned} \tag{4}$$

The integration is taken over a time span just around the detected pulse. Clearly, this method looses accuracy when a single pulse waveform is hard to distinguish, e.g. due to high noise level or to overlapping signal reflections. In a hypothetical situation of no attenuation by the cable, 100% signal transmission and constant sensor transfer function, (4) directly probes Q_{app} (except for a factor 2 since the PD propagates in two directions).

3 SYSTEM IDENTIFICATION

For identification of the complete cable connection, a signal injection method is adopted [4, 5]. Figure 3 shows the coupling scheme for injection at the near end, which is also accomplished by inductive coupling. The square block in Figure 3 represents the cable with length ℓ, characteristic impedance Z_c and propagation coefficient γ. The response on the injected current I_{inj} is detected at the near end (I_n through $Z_{l,n}$) as well as at the far end (I_f through $Z_{l,f}$). The coupling characteristics of the injection and detection coils are calibrated in a standard calibration loop before installation. Therefore, currents I_n and I_f are obtained by measuring V_n and V_f. From the coupling characteristics for injection and detection, the admittance of the near circuit Y_n and the transfer $H_{n,f}$ (=I_f/I_n) from near to far end can be determined:

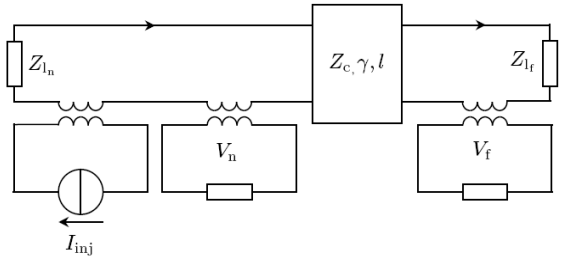

Figure 3: Coupling scheme for pulse injection at near cable end, and detection at far and near end.

$$\begin{aligned} &Y_n(\omega) = \frac{1}{Z_{l,n}(\omega) + Z_c}, \quad H_{n,f}(\omega) = T_f(\omega)\,\mathrm{e}^{-\gamma(\omega)\ell} \\ &\text{with} \quad T_f(\omega) = \frac{2Z_c}{Z_{l,f}(\omega) + Z_c} \end{aligned} \tag{5a}$$

In order to extract all parameters ($Z_{l,n}$, $Z_{l,f}$, Z_c and γ) also a signal needs to be injected at the far end [5], resulting in the far end admittance Y_f and the transfer $H_{f,n}$ from far to near end:

$$\begin{aligned} &Y_f(\omega) = \frac{1}{Z_{l,f}(\omega) + Z_c}, \quad H_{f,n}(\omega) = T_n(\omega)\,\mathrm{e}^{-\gamma(\omega)\ell} \\ &\text{with} \quad T_n(\omega) = \frac{2Z_c}{Z_{l,n}(\omega) + Z_c} \end{aligned} \tag{5b}$$

This method calls for detection units with an integrated signal injection source delivering sufficient energy in the frequency range relevant for PD diagnostics on power cables, i.e. up to about 5 MHz. As shown in [4], besides calibration, such injection circuit at both cable ends provides at the same time for an accurate time-base reference needed for accurate location of PDs.

4 COMPLEX CABLE CONNECTIONS

The PD calibration method described above takes into account the location of the PD and the effect of the RMU. It relies on having a good model for all relevant parameters. Efficiency of PD monitoring can be greatly enhanced by covering larger cable lengths, including RMUs. Signal transmission through these RMUs must be taken into account for PD magnitude calibration as well. Longer circuit lengths involve reduced signal levels both by losses from propagation along the cables and by attenuation from signal transmission through the RMUs. When an RMU has several outgoing cable connections the PD signal will spread over these channels, and the charge transferred into each of them is reduced.

4.1 Transmission single RMU

The impedance seen by a PD pulse arriving at an RMU differs from the characteristic impedance of the incoming cable. The voltage transfer function $H_{i\to j}(\omega)$ involves the (voltage) transmission coefficient from incoming cable i with impedance $Z_{c,i}$ to an impedance $Z^{(j)}(\omega)$ representing the load

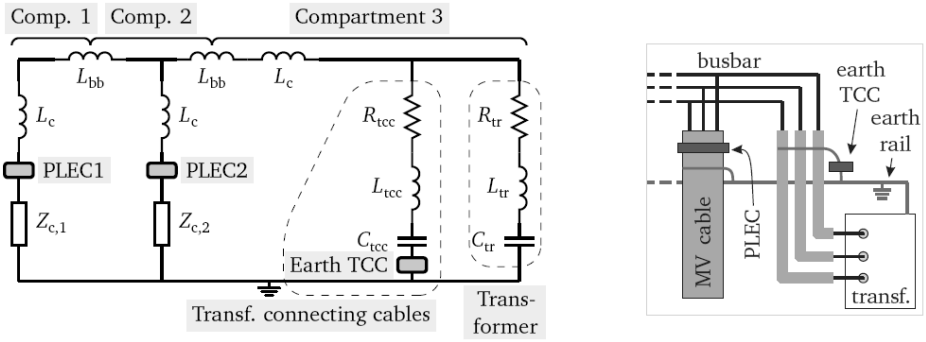

Figure 4: Equivalent circuit of RMU with two MV cables and transformer; sensor locations (PLEC) and earth of the transformer connecting cables (earth TCC) are indicated.

by the RMU and the transfer function $H_j(\omega)$ that describes the transfer to (one of) the outgoing cable(s), indicated with index *j*:

$$H_{i\to j}(\omega) = \frac{2}{Z_{c,i}/Z^{(i)}(\omega)+1}\cdot H_j(\omega) \qquad (6)$$

A compartment model [6] for an RMU with one incoming, one outgoing and a distribution transformer is shown in Figure 4. The cables in compartments 1 and 2 are modelled by their characteristic impedances; the transformer and the cables connecting the transformer are simulated as capacitances [6, 7]. The inductances and resistances in the equivalent circuit represent the contribution of the busbar connections to the overall impedance. An example of an experimental determined signal transfer in an RMU is shown in Figure 5. The black continuous line shows the measured signal transfer from incoming cable 1 (measured at PLEC1) to outgoing cable 2 (at PLEC2). Up to a frequency of about 1.5 MHz the transfer is close to unity. At higher frequencies resonances occur due to the transformer, its connecting cables and the circuit inductances. This is confirmed by the transfer from cable 1 to the earth screen of the cables connecting the transformer (measured at TCC, grey line). The dotted lines are model results based on fitted network parameters [6].

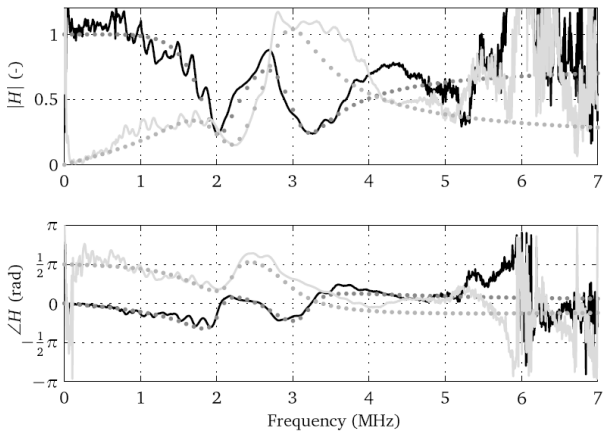

Figure 5: Measured (continuous) and simulated (dotted) transfer from PLEC1 to PLEC2 (black) and to TCC (grey), see Figure 4.

4.2 Transmission cascade of RMUs

The total transfer function for a compact RMU with two connected cables and a MV/LV transformer is calculated according to (6), using parameters based on measurements (like Figure 5) on a total of six RMUs. For frequencies up to 1 MHz the cable characteristic impedances are clearly lower than the impedance of the transformer including its connection to the busbar [6], and the transfer approaches one as observed in Figure 6 (black line). The effect of the transformer on the signal transfer can be neglected, $H_j(\omega)\approx 1$ in (6). The RMU impedance can be replaced by the equivalent parallel impedance of all outgoing cables. In this approximation the transfer to an RMU with an arbitrary number of connected cables becomes:

$$H_{i\to j}(\omega) = \frac{2}{Z_{c,i}\sum_{k\neq i} 1/Z_{c,k}^{(i)} + 1} = \frac{2}{Z_{c,i}\sum_{k} 1/Z_{c,k}^{(i)}} \qquad (7)$$

Here, $Z_{c,k}^{(i)}$ is the characteristic impedance of the k^{th} cable connected to RMU (*i*) and $Z_{c,i}$ indicates the characteristic impedance of the cable with the incoming signal to this RMU. For a composite cable connection, consisting of cables with length ℓ_i covering *N* RMUs each with n_i connected cables, the current transfer is:

$$H_{tot}(\omega) = \prod_{i=1}^{N} \frac{Z_{c,i}}{Z_{c,j}} H_{i\to j}\, \mathrm{e}^{-\gamma_i(\omega)\ell_i} = \prod_{i=1}^{N} \frac{2\,\mathrm{e}^{-\gamma_i(\omega)\ell_i}}{Z_{c,j}\sum_{k=1}^{n_i} 1/Z_{c,k}^{(i)}} \qquad (8)$$

The ratio of the characteristic impedance of incoming and outgoing cable included in (8) translates the signal voltage ratio in $H_{i\to j}(\omega)$ to the signal current ratio expressed in $H_{tot}(\omega)$. Taking all cable characteristics equal, with total cable length ℓ, (8) reduces to:

$$H_{tot}(\omega) = \mathrm{e}^{-\gamma(\omega)\ell} \prod_{i=1}^{N} \frac{2}{n_i} \qquad (9)$$

For RMUs with only one incoming and one outgoing cable (n_i=2) there is hardly any additional signal loss below 1 MHz. All incoming cables are more or less characteristically terminated by the

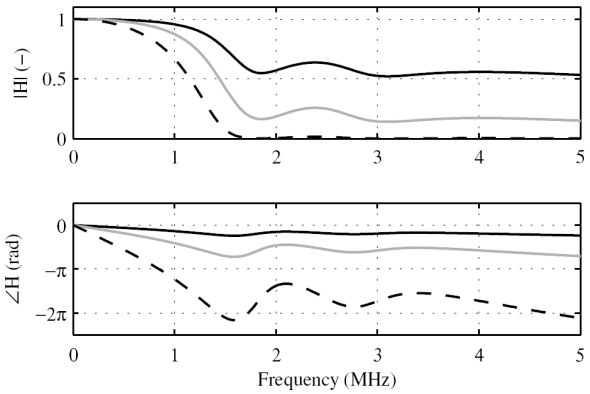

Figure 6: Transfer function by 1 (black line), 3 (grey line), and 9 (dashed line) RMUs.

outgoing cable. Signal attenuation occurs if there are more than two connected cables, which is accounted for by (9), and by the losses in the cable itself. The total transfer functions for three and nine RMUs are included in Figure 6 (grey, respectively dashed line). It is concluded that even for up to ten RMUs, each with one incoming and one outgoing cable, the signal is only halved at 1 MHz. The attenuation increases fast above this frequency.

4.3 Three-phase cables

PD signal excitation in a three-phase cable with one common earth screen results in induced apparent charge in all conductors. The amount of charge involved depends on the defect position within the cross section of the cable insulation. Sensor positions as indicated in Figure 4 (right) only probes the apparent charge induced in the earth screen [2, 8]. For a PD mainly concentrated between one of the phase conductors and the earth screen the situation is comparable to a PD in a single-phase cable. However, when the PD occurs between phase conductors, only a minor amount of charge is induced in the earth screen. PD sensitivity is low unless detection occurs at each phase conductor separately.

In a symmetric conductor arrangement as for the cable shown in Figure 7, two distinct propagation modes exist [8]. The mode detected with one sensor at the PLEC-position in Figure 4 probes the phase to shield mode, i.e. the mode corresponding to the sum of the PD currents in the three phases, returning via the earth shield. The phase to phase modes involve differences between two phase currents. The modes have different attenuation and propagation velocity characteristics. This may further affect the apparent charge distribution detected at the cable end [2].

5 CIRCUIT LENGTH AND SENSITIVITY

Whether PD diagnosis on long circuit lengths is feasible depends on the required sensitivity. This involves two a priori uncertain factors: (i) the noise level at a specific location, and (ii) the magnitude of the PDs produced by the defect. The noise level is

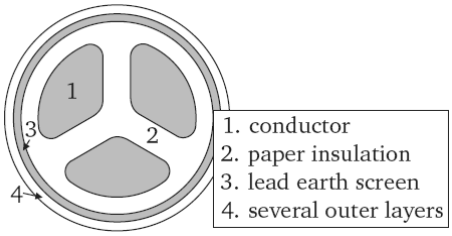

Figure 7: Three-phase cable with common earth screen (PILC: paper insulated lead covered).

determined by the local environment of the cable circuit. Its effect can partly be mitigated by sensor shielding, by choosing proper places inside the RMU to install the sensors, and by adequate signal processing techniques [5, 9-10]. The PD level depends on the nature of the defect and the type of component involved. With longer cables, PD signals attenuate stronger and the risk to miss PD activity from an upcoming fault increases. Either the defect is completely overlooked or it is detected in a later stage when it evolves, leaving less time for remedial action. Therefore, practical experience is essential to see whether the detection sensitivity remains sufficient to apply the PD location technique to long cable circuits.

The mapping of a circuit of 5561 m XLPE cable covering three RMUs is shown in Figure 8. The circuit shows small PD discharge concentrations during a few days at a joint positioned at 4022 m. After the increase of PD activity during three consecutive days it was decided to take the cable out of service and to replace the joint at the located position (overheated connector, an extensive analysis is given in [11]). This example points out that detectable PD activity sometimes is only temporarily present, indicating the importance of on-line diagnostics. With occasional off-line testing this kind of defect remains quite certainly undetected. The PD magnitudes from the defect hardly exceeded the overall noise level, but could be observed owing to their concentration. If this defect had occurred in a longer cable the first activity may have been observed in a later stage or even not at all. Apparently, for this type of defect in relation to the observed noise level, the detection probability becomes critical for XLPE cable lengths in excess of 6 km. Other defect types may have

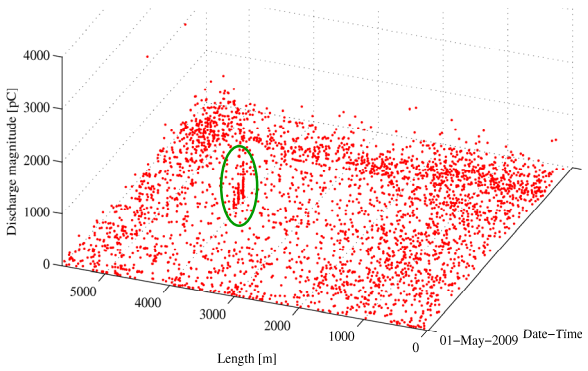

Figure 8: Mapping diagram of 5561 m (including three RMUs) with concentration at 4022 m.

typical PD magnitudes allowing longer or shorter maximum cable lengths to achieve fault detection with acceptable reliability.

6 DISCUSSION AND CONCLUSION

Calibration of PD magnitudes for on-line monitoring of energised cable connection is feasible. From the transfer of injected pulses at both ends, a model can be constructed providing information on PD signal attenuation and distortion before detection. The presented method assumed inductive coupling, but the method can be adapted to process capacitively detected signals. In principle, the model parameters can be measured when the cable is off-line. However, after reconnecting the cable to the grid the changed impedance due to the connected RMU should be accounted for.

The presented model is a simplification, and the parameters involved have an uncertainty margin. This makes that the calibration provides only an estimate. Continuous monitoring does not require a very high accuracy for correct risk assessment of detected PD activity, because different defect types will have a certain range of associated PD magnitudes. The method takes into account that sensitivity of PD detection drops with cable length and the number of RMUs in the connection.

For RMUs, with one incoming and one outgoing cable, signals are hardly affected for frequencies up to 1 MHz. Since the detection bandwidth for monitoring long cables is limited to about this frequency anyway due to signal attenuation, RMUs hardly contribute to loss in sensitivity for diagnosing long cable lengths. For instance three RMUs will result in over -3 dB attenuation as from 1.3 MHz according to Figure 6. One kilometre of XLPE cable already has a stronger effect, see Figure 1. The proposed calibration method takes these factors into account.

Sensitivity of cable diagnostics is fundamentally limited by the signal to noise ratio. Besides finding the best sensor position and proper shielding measures, signal processing techniques are applied to distinguish real PD signals from signal disturbances. In addition, two-sided detection allows rejecting all signals which have no possible counterparts from the sensor at the other end within the signal travelling time over the circuit length. The sensitivity settings must be optimised for any specific situation. For Figure 8 the detection level was lowered until the background of false PD detection started to become dominant.

7 ACKNOWLEDGMENTS

The authors wish to thank KEMA Nederland B.V. and the Dutch utilities Liander N.V., Stedin B.V. and Enexis B.V. for supporting this research.

8 REFERENCES

[1] F.H. Kreuger, “Partial discharge detection in high-voltage equipment”, Butterworths, 1989.

[2] P.A.A.F. Wouters, “On-line calibration of high-frequency partial discharge signals in three-phase belted power cables”, IEE Proceed. Sci., Meas. and Techn., vol. 152, no. 2, pp. 79-86, Mar 2005.

[3] Steven A. Boggs, “Partial discharge – part II: detection sensitivity”, IEEE EI Magazine, vol. 6, no. 5, pp. 35-42, Sep/Oct 1990.

[4] P.C.J.M. van der Wielen, J. Veen, P.A.A.F. Wouters, E.F. Steennis, “On-line partial discharge detection of MV cables with defect localisation (PDOL) based on two time synchronised sensors”, 18th Int. Conf. Electr. Distrib. (CIRED), Session 1, Turin, Jun 2005.

[5] J. Veen, “On-line Signal Analysis of Partial Discharges in Medium-Voltage Power Cables”, thesis Eindhoven University of Technology, Apr 2005.

[6] P. Wagenaars, P.A.A.F. Wouters, P.C.J.M. van der Wielen, E.F. Steennis, “Influence of ring-main-units and substations on online partial discharge detection and location in medium-voltage cable networks”, IEEE Trans. Power Delivery, vol. 26, no. 2, pp. 1064-1071, Apr 2011.

[7] B.T. Phung, T.R. Blackburn, W.W. Lay, “Partial discharge location in transformer windings”, 13th Int. Symp. High-voltage Eng. (ISH), Delft, Aug 2003.

[8] P. Wagenaars, P.A.A.F. Wouters, P.C.J.M. van der Wielen, E.F. Steennis, “Measurement of transmission line parameters of three-core power cables with common earth screen”, IET Proceed. Sci., Meas. & Techn., vol. 4, no. 3, pp. 146-155, May 2010.

[9] I. Shim, J.J. Soraghan, and W.H. Siew, “Digital signal processing applied to the detection of partial discharge: An overview”, IEEE EI Magazine, vol. 16, no. 3, pp. 6-12, May/Jun 2000.

[10] Hao Zhang, T.R. Blackburn, B.T. Phung and D. Sen, “A Novel Wavelet Transform Technique for On-Line Partial Dicharge Measurements Part 1: WT De-noising Algorithm”, IEEE Trans. Dielectr. Electr. Insul., vol. 14, no. 1, pp. 3-14, Feb 2007.

[11] S. Mousavi Gargari, P.A.A.F. Wouters, P.C.J.M. van der Wielen, E.F. Steennis, “Partial discharge parameters to evaluate the insulation condition in medium voltage cable networks”, accepted for publication in IEEE Trans. Dielectr. Electr. Insul., 2011.